

# Internal Wave Excitation by Turbulent Convection

D. Lecoanet<sup>1</sup>, M. Le Bars<sup>2,3</sup>, K. J. Burns<sup>4</sup>, E. Quataert<sup>1</sup>, G. M. Vasil<sup>5</sup>,  
B. P. Brown<sup>6</sup> & J. S. Oishi<sup>7</sup>

<sup>1</sup>University of California, Berkeley, USA

<sup>2</sup>IRPHE, Marseille, France

<sup>3</sup>University of California, Los Angeles, USA

<sup>4</sup>MIT, Cambridge, USA

<sup>5</sup>University of Sydney, Sydney, Australia

<sup>6</sup>University of Colorado, Boulder, USA

<sup>7</sup>Farmingdale State College, Farmingdale, USA

## Abstract

Convection near a stably stratified region can excite internal gravity waves. This occurs in a wide range of geophysical settings, including the Earth's atmosphere and core, as well as in astrophysical systems like some gas giants like Saturn, and most stars including the sun. In each of these circumstances, the wave excitation mechanism and subsequent wave energy flux spectrum is of great interest. In this work, we study both the excitation mechanism and the wave energy flux spectrum by a combination of experiments and numerical simulations. We find the waves are excited in the bulk of the convective region. Preliminary comparisons to analytic predictions of the wave energy flux are presented.

## 1 Introduction

In nature, it is not unusual to find stably stratified fluid adjacent to convectively unstable fluid. This can occur in the Earth's atmosphere, where the troposphere is convective and the stratosphere is stably stratified; in lakes, where surface solar heating can drive convection above stably stratified fresh water; in the oceans, where geothermal heating can drive convection near the ocean floor, but the water above is stably stratified due to salinity gradients; possible in the Earth's liquid core (Hirose et al., 2013), where gradients in thermal conductivity and composition diffusivities maybe lead to different layers of stable or unstable liquid metal; and, in stars, as most stars contain at least one convective and at least one radiative (stably stratified) zone.

Internal waves can play a dynamically important role via nonlocal transport. Momentum transport by convectively excited internal waves is thought to generate the quasi-biennial oscillation of zonal wind in the equatorial stratosphere (Baldwin et al., 2001), an important physical phenomenon used to calibrate global climate models. Angular momentum transport by convectively excited internal waves may play a crucial role in setting the initial rotation rates of neutron stars (Fuller et al., 2015). In the last year of life of a massive star, convectively excited internal waves may transport even energy to the surface layers to unbind them, launching a wind (Quataert and Shiode, 2012). In each of these cases, internal waves are able to transport some quantity—momentum, angular momentum, energy—across large, stable buoyancy gradients. Thus, internal waves represent an important, if unusual, transport mechanism.

The nonlocal transport by internal waves depends on the amplitude of the excited waves, as well as what type of waves are excited. For instance, in some astrophysical contexts, only the highest frequency waves can propagate far enough to lead to interesting transport (Fuller et al., 2014). The literature also includes various proposed mechanisms

for the generation of internal waves by convection, including: the obstacle effect; the mechanical oscillator effect; and bulk forcing (e.g., Ansong and Sutherland, 2010, and references within).

In the following, we will study the mechanism of wave excitation by convection, and present preliminary results on the wave energy flux spectrum. In section 2 we describe our experimental results (based on Le Bars et al., 2015). Section 3 shows the results of simulations inspired by the experiment (based on Lecoanet et al., 2015). These simulations suggest the wave excitation is primarily via Reynolds stresses within the bulk of the convection zone. Section 4 briefly summarizes a theoretical prediction of the wave energy flux made in Lecoanet and Quataert (2013). Finally, in section 5, we discuss wave energy flux spectra from new 3D numerical simulations, and how they agree or disagree with the theory.

## 2 Water Experiment

We have performed experiments of internal wave excitation by convection using water's unusual property that its density maximum is at 4°C (Le Bars et al., 2015). This type of experiment was first reported by Townsend (1964), but benefits greatly from modern measurement and analysis techniques. The experimental setup is shown in figure 1(a). It consists of a rectangular tank with internal dimensions of 18 cm by 4 cm in width and 34 cm in height. The lower and upper boundaries kept at fixed temperature of 0°C and 22°C respectively by circulating thermostated baths. We perform high sensitivity temperature measurements, and velocity measurements using PIV. Because water's density maximum is at 4°C, the water is convective from the bottom of the tank to the 4°C isotherm, and then stably stratified above. PIV measurements show the convection in the lower part of the tank is organized into a large scale circulation with upflow in the center of the tank, superimposed with plumes emitted from the bottom boundary.

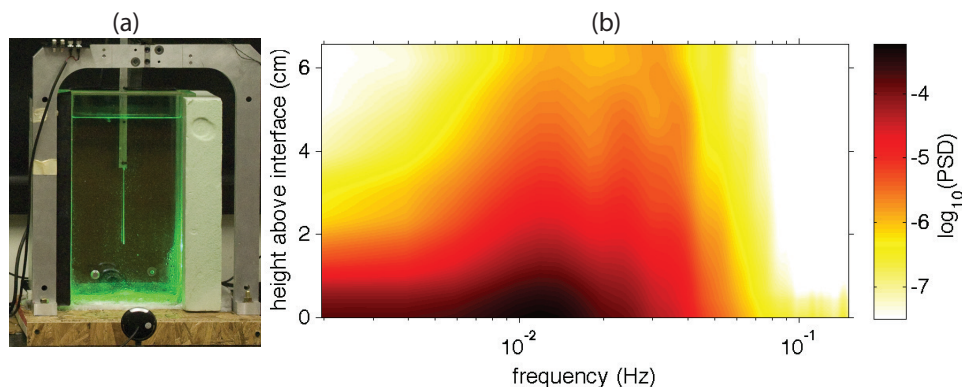


Figure 1: (a) Picture of experimental setup, showing the tank, two thermistor probes, and a green laser sheet used for PIV measurements. (b) Spectrogram of the horizontal velocity squared in the stratified region, measured by PIV over 13 minutes.

Figure 1(b) shows the power as a function of height above the convective-stably stratified interface, and as a function of frequency. The buoyancy frequency in the stable region is about 0.07Hz. As expected, there is very little wave energy at frequencies higher than the buoyancy frequency. Near the interface, most of the wave energy is carried by low frequency waves with frequencies  $\sim 0.01\text{Hz}$ , similar to the frequency of the large scale circulation in the convection zone. However, these low frequency waves preferentially damp

(due to viscosity) as they propagate upward, leaving mostly high frequency waves near the top of the measurement region.

### 3 Simulations of Water Experiment

We have run numerical simulations (Lecoanet et al., 2015) inspired by the experiment described in section 2. The simulations were run in the pseudo-spectral code Dedalus (Burns et al., 2017, see [dedalus-project.org](http://dedalus-project.org) for more information). The simulations are 2D, as the tank is very thin in one direction. The statistical properties of the simulated flow are qualitatively similar to those of the experiment. In particular, we plot the spectrogram of the waves in the stably stratified region in figure 2(a), which qualitatively matches the experimental spectrogram in figure 1(b). One qualitative difference between the simulations and the experiment is that the simulations have upflows on the sides, due to our use of free-slip, no flux horizontal boundary conditions for computational convenience.

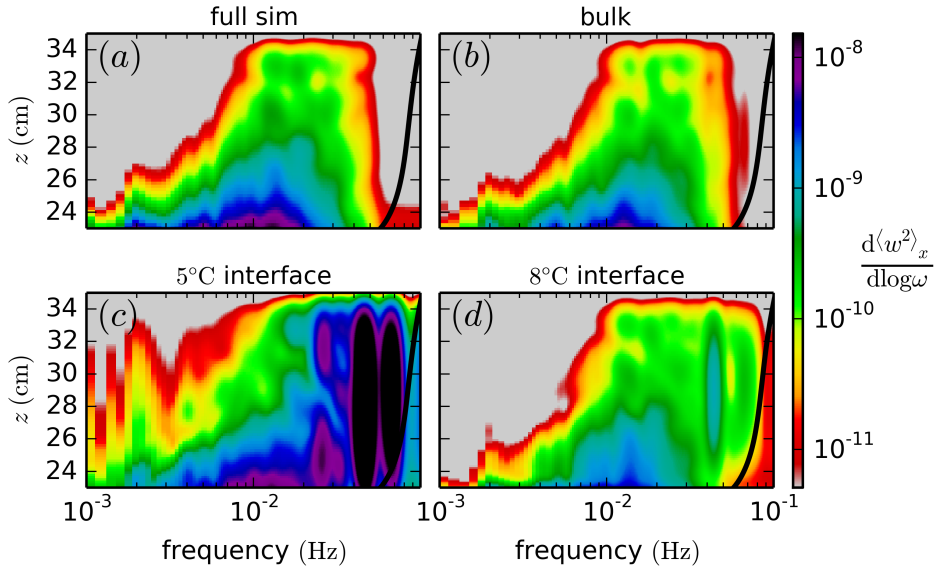


Figure 2: Spectrograms of the vertical velocity squared in the stable region of four different simulations: (a) The simulation of the experiment; (b) The model simulation using the bulk forcing model; (c) & (d) The model simulations using the interface forcing model, using the 5°C and 8°C isotherms as the interface, respectively.

To try to determine the mechanism behind the wave excitation, we ran several model simulations testing different theories. We studied the mechanical oscillator effect (i.e., interface forcing), and bulk forcing theories. To test the bulk forcing theory, we solved the forced linear wave equation

$$\nabla^2 (\partial_t - \nu \nabla^2) \partial_t \xi_z + N^2 \partial_x^2 \xi_z = S, \quad (1)$$

where  $\xi_z$  is the vertical wave displacement,  $S$  is a convective source term related to the Reynolds stresses within the convection zone, and all the other symbols have their usual meaning. We solved this equation with the source term  $S$  calculated directly from the full simulation at every time and position within the convection zone. To test the interface forcing theory, we solved, the unforced linear wave equation,

$$\nabla^2 (\partial_t - \nu \nabla^2) \partial_t \xi_z + N^2 \partial_x^2 \xi_z = 0, \quad (2)$$

subject to the boundary condition that the vertical displacement is equal to the interface position at the bottom of the stable region. In this case, we calculate the interface position from the full simulation at every time, using the interface definition of either the 5°C and 8°C isotherm.

Each of our three model simulations makes a prediction of the wave field in the stable region. Figure 2 shows the statistical properties of these waves. It shows that bulk forcing via Reynolds stresses is a very accurate description of the wave excitation process, but interface forcing is less accurate. Using the higher 8°C interface definition is more accurate because the motions are mostly linear at that height, and thus the simulation is mostly of wave propagation rather than wave generation. The bulk forcing simulation matches the wave phase in addition to the wave spectrum.

#### 4 Wave Energy Flux Predictions

Now that we have verified the bulk forcing mechanism of wave excitation, we can try to use it to make theoretical predictions of the spectrum of wave energy flux. Following Goldreich and Kumar (1990), in Lecoanet and Quataert (2013) we estimated the wave energy flux by assuming the waves are excited by the superposition of independent eddies, with sizes  $h$  and lifetimes  $\tau$  which satisfy the Kolmogorov cascade ansatz,  $h \sim \tau^{3/2}$ . Assuming a sharp transition between the convective and stable regions, this predicts a wave energy flux spectrum of

$$\frac{dF}{d \log \omega d \log k_{\perp}} \sim F_c \mathcal{M} (k_{\perp} H)^4 \left( \frac{\omega}{\omega_c} \right)^{-13/2}. \quad (3)$$

This expression gives the differential wave flux as a function of the wave frequency  $\omega$ , and its horizontal wavenumber  $k_{\perp}$ .  $F_c$  is the convective flux,  $H$  is the height of the convection zone (or largest convective motions),  $\omega_c$  is a convection frequency.  $\mathcal{M} = \omega_c/N_0$  is the convective Mach number, where  $N_0$  is a characteristic buoyancy frequency in the stable region. This expression is valid for  $\omega > \omega_c$ , and  $k_{\perp} \lesssim H^{-1}(\omega/\omega_c)^{3/2}$ . Outside of this region, we expect little wave energy flux.

This expression predicts that the most efficiently excited waves have the same (horizontal) size and frequency as the energy-bearing convective motions. The total wave flux is smaller than the convective flux by  $\mathcal{M}$ . At a fixed horizontal lengthscale, the wave flux drops quickly with  $\omega$ , because the waves can only be excited by the incoherent superposition of many small scale eddies which match the frequency  $\omega$ . This is inefficient because on average the small scale eddies will cancel out, and each individual eddy does not carry much energy.

#### 5 Wave Energy Flux in 3D Simulations

We now test the prediction of equation 3 against numerical simulations. We cannot compare directly to the simulations of section 3 because the 2D convection does not satisfy the Kolmogorov cascade assumption, whereas high resolution 3D convection simulations and experiments do seem to have a Kolmogorov cascade (Lohse and Xia, 2010; Kumar et al., 2014).

We run 3D simulations of the fully compressible Navier-Stokes equations. We implicitly timestep over the sound waves so we can still run at low Mach number ( $\sim 0.01$ ) without being limited by a stringent CFL condition (Lecoanet et al., 2014). The simulations are initialized to have a convection zone in the upper part of the domain, and a

stable region below. The initial thermal state is fixed, but nonlinear perturbations around it can (and do) develop. We use temperature diffusion on the temperature fluctuations, using a constant thermal diffusivity (with units of  $\text{cm}^2/\text{s}$ ). We have a fixed temperature bottom boundary condition, and fixed flux top boundary condition. We run the simulations until they are in approximate flux equilibrium, about a thermal time across the domain.

We will only describe one simulation, which was run with a convection zone of size  $\sim 3$  density scale heights, with  $\text{Ra} = 10^7$ ,  $\text{Pr} = 1$ ,  $\text{Ma} \sim 0.01$ , and a resolution of  $256^3$  modes. Because the convection zone comprises multiple density scaleheights, the convective plumes are mostly at small scales at the top of the domain, and merge to larger scales as they descend toward the stable region. This places stringent resolution limits on the simulation near the top of the domain.

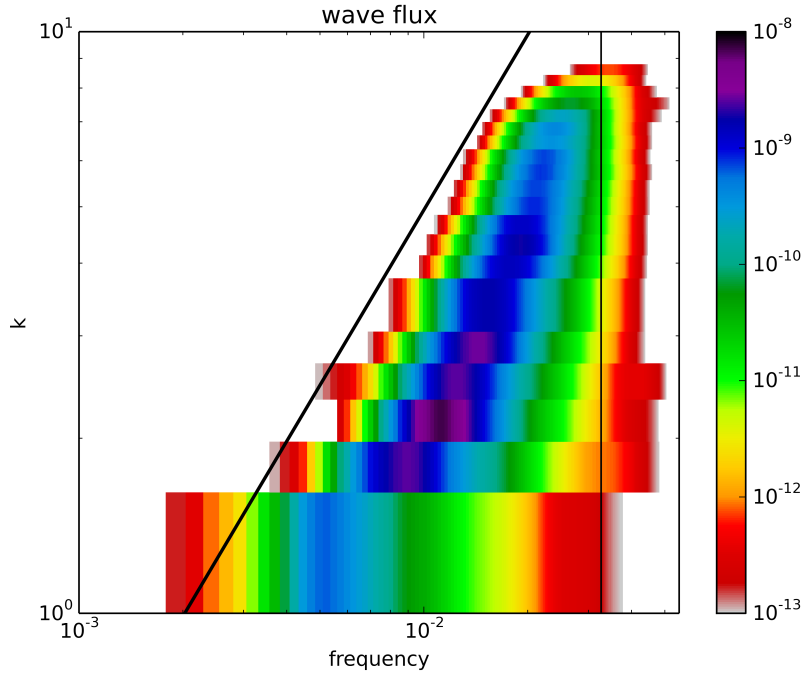


Figure 3: Wave energy flux as a function of perpendicular wavenumber  $k$  and frequency  $f = \omega/(2\pi)$ . The thin black line is the buoyancy frequency in the stable region. The thick black line is the line  $k = \omega/u_c$ , showing the “sweeping” wavenumber. To build statistics, the spectrum has been smoothed with a gaussian filter with width 0.1 decades in both wavenumber and frequency.

In figure 3, we plot the wave energy flux as a function of  $k$  and frequency. We calculate the wave flux by calculating  $wp'$  at various heights, where  $p'$  is the pressure perturbation field. The wave amplitude, and thus  $wp'$ , falls off exponentially in the stable region due to wave damping from viscosity and thermal diffusivity. We fit this curve to an exponential, and interpolate the value of  $wp'$  to the interface between the convective and stably stratified region, which is the height at which we calculate the spectrum.

Because the simulation is not very turbulent, and because the generated waves are close to the buoyancy frequency, we can neither confirm nor refute the specific details of equation 3. Nevertheless, we can directly compare to certain aspects of the theory. We predict that the highest wavenumbers excited for a given frequency is  $k_{\perp\text{max}} \sim H^{-1}(\omega/\omega_c)^{3/2}$ . However, our spectrum has a sharp cutoff at  $k_{\perp} \sim \omega$ . This contradicts the theory proposed

in Lecoanet and Quataert (2013).

We now propose a resolution to this discrepancy. If small-scale convective eddies (responsible for exciting high  $k$  waves) are advected by the large-scale convective flow, we expect the waves they generate to be doppler shifted by  $\omega \rightarrow \omega + u_c k_\perp$ , where  $u_c$  is the horizontal convective velocity. In this case, all waves which we predict to have frequencies less than  $u_c k$  should be doppler shifted up to that frequency. Higher frequency waves should be unaffected. This predicts that energy should accumulate at  $\omega$  and  $k$  satisfying  $k = \omega/u_c$ . We plot this line in figure 3, using the rms horizontal velocity near the bottom of the convection zone as an estimate for  $u_c$ . This velocity is about a factor of two smaller than it would need to be to explain our spectrum. Nevertheless, we believe wave excitation by “sweeping” eddies along the bottom of the convection zone is an important physical effect neglected in previous work.

One can calculate the expected energy flux along the line  $k = \omega/u_c$  by doppler shifting equation 3. The prediction is for the flux to drop as  $k^{-1/3}$ . This simulation shows a much sharper drop with  $k$ . However, this maybe related to our limited inertial range and/or proximity to the buoyancy frequency. We also still predict that the flux should drop very sharply—as  $\omega^{-13/2}$ —for our lowest  $k$  waves. Our spectrum is consistent with this decrease, but only for low  $k$ . As  $k$  increases, the power law exponent appears to steepen. It is likely the proximity to the buoyancy frequency plays an important role in the decrease in flux at high frequencies. Nevertheless, we find these results promising.

## References

- Ansorg, J. K. and Sutherland, B. R. (2010). Internal gravity waves generated by convective plumes. *Journal of Fluid Mechanics*, 648:405.
- Baldwin, M. P., Gray, L. J., Dunkerton, T. J., Hamilton, K., Haynes, P. H., Randel, W. J., Holton, J. R., Alexander, M. J., Hirota, I., Horinouchi, T., Jones, D. B. A., Kinnnersley, J. S., Marquardt, C., Sato, K., and Takahashi, M. (2001). The quasi-biennial oscillation. *Reviews of Geophysics*, 39:179–230.
- Burns, K. J., Vasil, G. M., Oishi, J. S., Lecoanet, D., Brown, B. P., and Quataert, E. (2017). Dedalus: A Flexible Pseudo-Spectral Framework for Solving Partial Differential Equations. In preparation.
- Fuller, J., Cantiello, M., Lecoanet, D., and Quataert, E. (2015). The Spin Rate of Pre-collapse Stellar Cores: Wave-driven Angular Momentum Transport in Massive Stars. *ApJ*, 810:101.
- Fuller, J., Lecoanet, D., Cantiello, M., and Brown, B. (2014). Angular Momentum Transport via Internal Gravity Waves in Evolving Stars. *ApJ*, 796:17.
- Goldreich, P. and Kumar, P. (1990). Wave generation by turbulent convection. *ApJ*, 363:694–704.
- Hirose, K., Labrosse, S., and Hernlund, J. (2013). Composition and State of the Core. *Annual Review of Earth and Planetary Sciences*, 41:657–691.
- Kumar, A., Chatterjee, A. G., and Verma, M. K. (2014). Energy spectrum of buoyancy-driven turbulence. *Phys. Rev. E*, 90(2):023016.

- Le Bars, M., Lecoanet, D., Perrard, S., Ribeiro, A., Rodet, L., Aurnou, J. M., and Le Gal, P. (2015). Experimental study of internal wave generation by convection in water. *Fluid Dynamics Research*, 47(4):045502.
- Lecoanet, D., Brown, B. P., Zweibel, E. G., Burns, K. J., Oishi, J. S., and Vasil, G. M. (2014). Conduction in Low Mach Number Flows. I. Linear and Weakly Nonlinear Regimes. *ApJ*, 797:94.
- Lecoanet, D., Le Bars, M., Burns, K. J., Vasil, G. M., Brown, B. P., Quataert, E., and Oishi, J. S. (2015). Numerical simulations of internal wave generation by convection in water. *Phys. Rev. E*, 91(6):063016.
- Lecoanet, D. and Quataert, E. (2013). Internal gravity wave excitation by turbulent convection. *MNRAS*, 430:2363–2376.
- Lohse, D. and Xia, K.-Q. (2010). Small-Scale Properties of Turbulent Rayleigh-Bénard Convection. *Annual Review of Fluid Mechanics*, 42:335–364.
- Quataert, E. and Shiode, J. (2012). Wave-driven mass loss in the last year of stellar evolution: setting the stage for the most luminous core-collapse supernovae. *MNRAS*, 423:L92–L96.
- Townsend, A. A. (1964). Natural convection in water over an ice surface. *Quarterly Journal of the Royal Meteorological Society*, 90:248–259.